

<https://doi.org/10.14379/iodp.proc.363.203.2020>



Contents

- 1 Abstract
- 1 Introduction
- 1 Site location and setting
- 2 Methods and materials
- 2 Results
- 2 Acknowledgments
- 2 References
- 4 Appendix

Data report: Miocene planktonic foraminifers *Dentoglobigerina* and *Globoquadrina* from IODP Sites U1489 and U1490, Expedition 363¹

Florent Fayolle² and Bridget S. Wade²

Keywords: International Ocean Discovery Program, IODP, *JOIDES Resolution*, Expedition 363, Pacific Warm Pool, Site U1489, Site U1490, planktonic foraminifers, Miocene

Abstract

International Ocean Discovery Program Expedition 363 Sites U1489 and U1490, located in the Western Pacific Warm Pool, contain diverse assemblages of planktonic foraminifers. We examined and imaged specimens of Miocene *Dentoglobigerina* and *Globoquadrina* to determine the presence or absence of spine holes and pustules in their wall texture. A total of 15 specimens were observed across six species, including *Dentoglobigerina baroemouensis*, *Dentoglobigerina binaiensis*, *Dentoglobigerina globosa*, *Dentoglobigerina globularis*, *Dentoglobigerina tripartita*, and *Globoquadrina dehiscens*. Here we present scanning electron microscope and z-stacking light microscope images in three views, including illustrations of their wall texture.

Introduction

Dentoglobigerina is a diverse genus of planktonic foraminifers that ranges from the middle Eocene to recent. The descendant genus *Globoquadrina* is currently monospecific, consisting of *Globoquadrina dehiscens* and ranging from the early to late Miocene (Wade et al., 2018). The taxonomy and biostratigraphy of Eocene and Oligocene *Dentoglobigerina* were reviewed by Olsson et al. (2006) and Wade et al. (2018), respectively, as part of the Paleogene Planktonic Foraminifera Working Group. However, the wall texture of Miocene *Dentoglobigerina* and *Globoquadrina* has not yet been examined in detail.

The dentoglobigerinids are a difficult group; in addition to morphological variability is the issue that the wall texture and the presence and absence of spine holes are highly variable across the lineage. Research to date has not been able to determine whether or not spines are a conservative trait in Miocene *Dentoglobigerina*. Spine holes have not been observed in all species of *Dentoglobigerina* (Wade et al., 2018), mostly because of the difficulty in finding well-preserved specimens and the considerable time needed to lo-

cate them under a scanning electron microscope (SEM). However, given that the identification of spine holes is not evident in some species, it was suggested by Pearson and Wade (2015) that there could be two clades with similar morphologies, one spinose and one nonspinose, or that spines could have been lost through evolution. Pustules are also of interest for this study because they are frequently seen in umbilical shoulders of *Dentoglobigerina* specimens. Here we contribute to the debate on Miocene *Dentoglobigerina* and *Globoquadrina* wall texture and taxonomy through light microscope (z-stacking) and SEM examination of specimens from Sites U1489 and U1490 in three views (umbilical, edge, and spiral). We also include wall texture images and record the presence or absence of spine holes and pustules around the umbilical area.

Site location and setting

Seven sites were cored in 2016 during International Ocean Discovery Program Expedition 363 in the Western Pacific Warm Pool (Figure F1). We examined two sites to record the presence of *Dentoglobigerina* and *Globoquadrina*: Site U1489 cored four holes at 3400 meters below sea level (mbsl), and Site U1490 cored three holes at 2300 mbsl (Rosenthal et al., 2018a). This data report focuses on the *Dentoglobigerina* and *Globoquadrina* genera found in lower to middle Miocene sediments. The geological age of the sediment samples ranges from 22.13 to 13.27 Ma according to the shipboard age model (Rosenthal et al., 2018a).

Site U1489 (02°07.19'N, 141°01.67'E) is situated on the western slope of the southern Eauripik Rise in the Caroline basin of Papua New Guinea (Figure F1; Rosenthal et al., 2018b). Site U1490 (05°48.95'N, 142°39.27'E) is located on the northern edge of the Eauripik Rise about 431 km north of Site U1489 (Figure F1; Rosenthal et al., 2018c). Of the seven total holes cored at Sites U1489 and U1490, Holes U1489D and U1490A are examined in the present study.

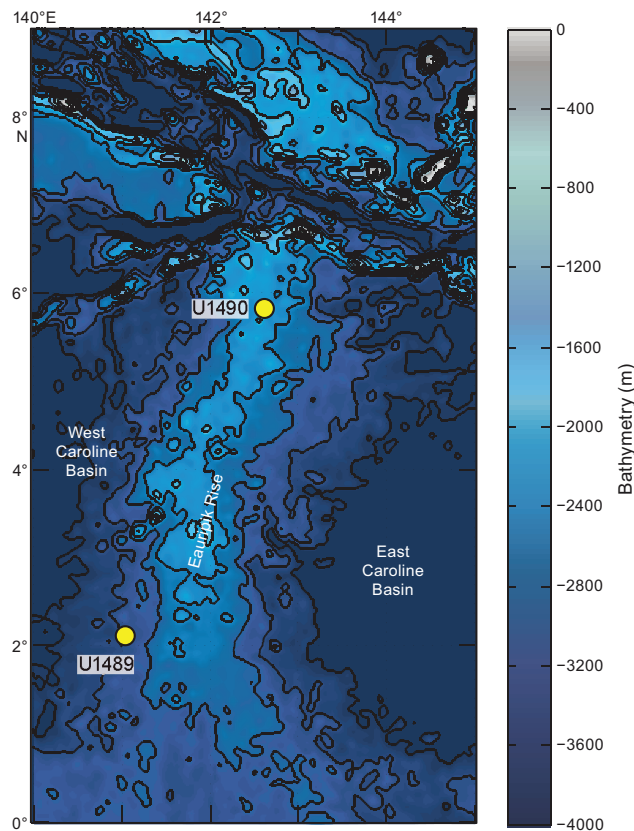
¹ Fayolle, F., and Wade, B.S., 2020. Data report: Miocene planktonic foraminifers *Dentoglobigerina* and *Globoquadrina* from IODP Sites U1489 and U1490, Expedition 363. In Rosenthal, Y., Holbourn, A.E., Kulhanek, D.K., and the Expedition 363 Scientists, *Western Pacific Warm Pool*. Proceedings of the International Ocean Discovery Program, 363: College Station, TX (International Ocean Discovery Program). <https://doi.org/10.14379/iodp.proc.363.203.2020>

² Department of Earth Sciences, University College London, UK. Correspondence author: florent.fayolle.18@alumni.ucl.ac.uk

MS 363-203: Received 12 February 2020 · Accepted 16 July 2020 · Published 13 November 2020

This work is distributed under the [Creative Commons Attribution 4.0 International](https://creativecommons.org/licenses/by/4.0/) (CC BY 4.0) license. 

Figure F1. Bathymetric map of the equatorial Pacific Ocean indicating locations of Site U1489 (02°07.19'N, 141°01.67'E; 3400 mbsl) and Site U1490 (05°48.95'N, 142°39.27'E; 2300 mbsl) on the Eauripik Rise in the Western Pacific Warm Pool. Contour interval = 500 m. Bathymetric data from Amante and Eakins (2009); figure modified from Rosenthal et al. (2018a).



Methods and materials

Sites U1489 and U1490 both recovered the lower and middle Miocene and were chosen for the relatively good preservation of planktonic foraminifers (Rosenthal et al., 2018b; Rosenthal et al., 2018c). Table T1 lists the samples analyzed, including their depth in the section and biostratigraphic age assignment. The site ages covered in this study were calibrated with the Miocene Planktonic Foraminiferal Zonation by Wade et al. (2011).

Dentoglobigerina and *Globoquadrina* specimens were picked manually from the residues of the >150 µm size fraction using a light microscope. A total of 15 specimens were selected across 5 samples based on their preservation. Images in three views (umbilical, edge, and spiral view) of the selected specimens were taken using an Olympus SZX10 z-stacking light microscope. A Jeol JSM-6480LV high-performance SEM from the UCL Earth Sciences laboratory was used to examine wall texture and assess the presence of morphological features, including spine holes and pustules, at higher resolution. Each stub was sputter-coated in an argon and gold atmosphere using a sputter-coater machine. Spine holes were investigated across the three views of each specimen's test, and the study focused on areas where pores were sufficiently preserved, pore ridges smooth, and not affected by diagenetic processes.

Table T1. Biostratigraphic and location details of studied samples, Sites U1489 and U1490. [Download table in CSV format.](#)

Table T2. Spinose characters and pustules of selected *Dentoglobigerina* and *Globoquadrina* specimens, Sites U1489 and U1490. [Download table in CSV format.](#)

Results

At least six species belonging to the genus *Dentoglobigerina*, including its descendant *G. dehiscens*, were identified in five samples from Holes U1489D and U1490A. Morphological features (pustules and spine holes) of the wall texture of each Miocene specimen are recorded in Table T2, and images of each specimen are illustrated in Plates P1–P15. Overall, the preservation of specimens from Hole U1489D is better than for Hole U1490A.

Acknowledgments

This research used samples provided by the International Ocean Discovery Program (IODP). Funding for this research was provided by Natural Environment Research Council grant number NE/P016642. We thank Jim Davy for assistance with SEM preparation and Marcin Latas for help with the z-stacking light microscope. The manuscript was improved by a review from Kirsty Edgar and comments from Denise Kulhanek. Florent Fayolle acknowledges funding from the Geologists' Association Curry Award.

References

- Amante, C., and Eakins, B.W., 2009. *ETOPO1 1 Arc-Minute Global Relief Model: Procedures, Data Sources and Analysis*. NOAA Technical Memorandum NESDIS NGDC-24. National Geophysical Data Center, NOAA. <https://doi.org/10.7289/V5C8276M>
- Bermúdez, P.J., 1961. Contribucion al estudio de las Globigerinidea de la region Caribe-Antillana (Paleocene-Reciente): Boletino Geologia (Venezuela). *Memoria Congres de Geologia Venezolano*, 3:1119–1393.
- Blow, W.H., 1979. The Cainozoic *Globigerinida*: A Study of the Morphology, Taxonomy, Evolutionary Relationships and the Stratigraphical Distribution of Some *Globigerinida* (mainly *Globigerinacea*): Leiden, The Netherlands (E.J. Brill).
- Bolli, H.M., 1957. The genera *Globigerina* and *Globorotaria* in Paleocene-lower Eocene Lizard Springs Formation of Trinidad, BWI. *Bulletin of the United States National Museum*, 215:61–81.
- Carpenter, W.B., Parker, W.K., and Jones, T.R., 1862. *Introduction to the Study of the Foraminifera*: London (R. Hardwicke). <https://doi.org/10.5962/bhl.title.9133>
- Chapman, E, Parr, W.J., and Collins, A.C., 1934. Tertiary foraminifers of Victoria, Australia: the Balcombian deposits of Port Philip (Pt. III). *Journal of the Linnean Society of London, Zoology*, 38(262):553–577. <https://doi.org/10.1111/j.1096-3642.1934.tb00996.x>
- d'Orbigny, A.D., 1826. Tableau methodique de la classe des Foraminifères. *Annales des Sciences Naturelles*, 7:245–314.
- Finlay, H.J., 1947. New Zealand Foraminifera: key species in stratigraphy – No. 5. *New Zealand Journal of Science and Technology*, 28:259–292.
- Fox, L.R., and Wade, B.S., 2013. Systematic taxonomy of early-middle Miocene planktonic foraminifera from the equatorial Pacific Ocean: Integrated Ocean Drilling Program, Site U1338. *Journal of Foraminiferal Research*, 43(4):374–405. <https://doi.org/10.2113/gsfjr.43.4.374>
- Koch, R., 1935. Namensänderung einiger Tertiär-Foraminiferen aus Neiderländisch Ost-Indien. *Eclogae Geologicae Helvetiae*, 28:557–558.

- Koch, R.E. 1926. Mitteltertiäre Foraminiferen aus Bulongan, Ost-Borneo. *Eclogae Geologicae Helvetiae*, 19(3):722–759.
- Leckie, R.M., Farnham, C., and Schmidt, M.G., 1993. Oligocene planktonic foraminifer biostratigraphy of Hole 803D (Ontong Java Plateau) and Hole 628A (Little Bahama Bank), and comparison with the southern high latitudes. In Berger, W.H., Kroenke, L.W., Mayer, L.A., et al. (Eds.), *Proceedings of the Ocean Drilling Program, Scientific Results*: College Station, TX (Ocean Drilling Program), 130:113–136.
<https://doi.org/10.2973/odp.proc.sr.130.012.1993>
- LeRoy, L.W., 1939. Some small foraminifera, Ostracoda and otoliths from the Neogene (Miocene) of the Rokan-Tapanoei area, central Sumatra. *Natuurkundig Tijdschrift voor Nederlandsch Indie*, 99(6):215–296.
- Olsson, R.K., Hemleben, C., and Pearson, P.N., 2006. Taxonomy, biostratigraphy, and phylogeny of Eocene *Dentoglobigerina*. In Pearson, P.N., Olsson, R.K., Huber, B.T., Hemleben, C., and Berggren, W.A. (Eds.), *Atlas of Eocene Planktonic Foraminifera*. Special Publication - Cushman Foundation for Foraminiferal Research, 41:401–412.
- Pearson, P.N., and Wade, B.S., 2009. Taxonomy and stable isotope paleoecology of well-preserved planktonic foraminifera from the uppermost Oligocene of Trinidad. *Journal of Foraminiferal Research*, 39(3):191–217.
<https://doi.org/10.2113/gsjfr.39.3.191>
- Pearson, P.N., and Wade, B.S., 2015. Systematic taxonomy of exceptionally well-preserved planktonic foraminifera from the Eocene/Oligocene boundary of Tanzania. *Special Publication - Cushman Foundation for Foraminiferal Research*, 45:1–85.
<https://discovery.ucl.ac.uk/id/eprint/1475039>
- Rosenthal, Y., Holbourn, A.E., Kulhanek, D.K., Aiello, I.W., Babila, T.L., Bayon, G., Beaufort, L., Bova, S.C., Chun, J.-H., Dang, H., Drury, A.J., Dunkley Jones, T., Eichler, P.P.B., Fernando, A.G.S., Gibson, K.A., Hatfield, R.G., Johnson, D.L., Kumagai, Y., Li, T., Linsley, B.K., Meinicke, N., Mountain, G.S., Opdyke, B.N., Pearson, P.N., Poole, C.R., Ravelo, A.C., Sagawa, T., Schmitt, A., Wurtzel, J.B., Xu, J., Yamamoto, M., and Zhang, Y.G., 2018a. Expedition 363 summary. In Rosenthal, Y., Holbourn, A.E., Kulhanek, D.K., and the Expedition 363 Scientists, *Western Pacific Warm Pool*. Proceedings of the International Ocean Discovery Program, 363: College Station, TX (International Ocean Discovery Program).
<https://doi.org/10.14379/iodp.proc.363.101.2018>
- Rosenthal, Y., Holbourn, A.E., Kulhanek, D.K., Aiello, I.W., Babila, T.L., Bayon, G., Beaufort, L., Bova, S.C., Chun, J.-H., Dang, H., Drury, A.J., Dunkley Jones, T., Eichler, P.P.B., Fernando, A.G.S., Gibson, K.A., Hatfield, R.G., Johnson, D.L., Kumagai, Y., Li, T., Linsley, B.K., Meinicke, N., Mountain, G.S., Opdyke, B.N., Pearson, P.N., Poole, C.R., Ravelo, A.C., Sagawa, T., Schmitt, A., Wurtzel, J.B., Xu, J., Yamamoto, M., and Zhang, Y.G., 2018b. Site U1489. In Rosenthal, Y., Holbourn, A.E., Kulhanek, D.K., and the Expedition 363 Scientists, *Western Pacific Warm Pool*. Proceedings of the International Ocean Discovery Program, 363: College Station, TX (International Ocean Discovery Program).
<https://doi.org/10.14379/iodp.proc.363.110.2018>
- Rosenthal, Y., Holbourn, A.E., Kulhanek, D.K., Aiello, I.W., Babila, T.L., Bayon, G., Beaufort, L., Bova, S.C., Chun, J.-H., Dang, H., Drury, A.J., Dunkley Jones, T., Eichler, P.P.B., Fernando, A.G.S., Gibson, K.A., Hatfield, R.G., Johnson, D.L., Kumagai, Y., Li, T., Linsley, B.K., Meinicke, N., Mountain, G.S., Opdyke, B.N., Pearson, P.N., Poole, C.R., Ravelo, A.C., Sagawa, T., Schmitt, A., Wurtzel, J.B., Xu, J., Yamamoto, M., and Zhang, Y.G., 2018c. Site U1490. In Rosenthal, Y., Holbourn, A.E., Kulhanek, D.K., and the Expedition 363 Scientists, *Western Pacific Warm Pool*. Proceedings of the International Ocean Discovery Program, 363: College Station, TX (International Ocean Discovery Program).
<https://doi.org/10.14379/iodp.proc.363.111.2018>
- Wade, B.S., Berggren, W.A., and Olsson, R.K., 2007. The biostratigraphy and paleobiology of Oligocene planktonic foraminifera from the equatorial Pacific Ocean (ODP Site 1218). *Marine Micropaleontology*, 62(3):167–179. <https://doi.org/10.1016/j.marmicro.2006.08.005>
- Wade, B.S., Pearson, P.N., Berggren, W.A., and Pälike, H., 2011. Review and revision of Cenozoic tropical planktonic foraminiferal biostratigraphy and calibration to the geomagnetic polarity and astronomical time scale. *Earth-Science Reviews*, 104(1–3):111–142.
<https://doi.org/10.1016/j.earscirev.2010.09.003>
- Wade, B.S., Pearson, P.N., Olsson, R.K., Fraass, A.J., Leckie, R.M., and Hemleben, C., 2018. Taxonomy, biostratigraphy, and phylogeny of Oligocene and lower Miocene *Dentoglobigerina* and *Globoquadrina*. In Wade, B.S., Olsson, R.K., Pearson, P.N., Huber, B.T., and Berggren, W.A. (Eds.), *Atlas of Oligocene Planktonic Foraminifera*. Special Publication - Cushman Foundation for Foraminiferal Research, 46:331–384.
<https://discovery.ucl.ac.uk/id/eprint/10049514>

Appendix

Systematic paleontology of selected taxa

Order Foraminiferida d'Orbigny, 1826

Superfamily Globigerinoidea Carpenter, Parker and Jones, 1862

Family Globigerinidae Carpenter, Parker & Jones, 1862

Genus *Dentoglobigerina* Blow, 1979

Dentoglobigerina baroemouensis (LeRoy, 1939)

(Plate **P1**, **P2**, **P3**, **P4**)

Globigerina baroemouensis, LeRoy (1939), p. 263, pl. 6, figs. 1–2

Dentoglobigerina baroemouensis, Wade et al. (2018), p. 335–338, pl. 11.1

Remarks: Wade et al. (2018) showed evidence for spine holes in *D. baroemouensis* (pl. 11.1, fig. 12), but these were not observed by Fox and Wade (2013) (fig. 5.1c). In this report, we present additional evidence in Plate **P1G–P1J** with specimen S1 showing several spine holes at pore intersections in the umbilical, edge, and spiral views. One spine hole is also observed in the edge view of specimen S2 in Plate **P2H**. These features were found in isolated areas, mostly over the last chamber near (1) the apertural shoulders and (2) at the intersection of chambers in the spiral view. In contrast, specimens from Plates **P3** and **P4** did not reveal any spine holes because recrystallization and calcite overgrowth heavily obscure pore intersections. All the specimens lack pustules in the umbilical region. *D. baroemouensis* was recorded in Subzone M1b and Zones M8 and M9.

Dentoglobigerina binaiensis (Koch, 1935)

(Plates **P5**, **P6**)

Globigerina binaiensis, Koch (1935), p. 558, *nomen novum* for *G. aspera* Koch (1926)

Dentoglobigerina binaiensis, Wade et al. (2018), p. 338–342, pl. 11.3

Remarks: Wade et al. (2018) reported evidence for spine holes in *D. binaiensis* (pl. 11.3, figs. 4, 8, 12), but these were not observed by Fox and Wade (2013) (fig. 5.3b). In this report, specimens illustrated in Plates **P5** and **P6** did not reveal any spine holes, even though they are well preserved as illustrated by the smooth and well-defined pores and pore ridges. Specimen S5 is highly pustulose in the apertural region (Plate **P5A**, **P5D**) and to a lesser extent in the edge view (Plate **P5B**, **P5E**). Specimen S6 shows aligned pustules (Plate **P6A**) on the final chamber, which are particularly apparent in edge view (Plate **P6E**). *D. binaiensis* was recorded in Zone M3.

Dentoglobigerina globosa (Bolli, 1957)

(Plates **P7**, **P8**, **P9**)

Globoquadrina altispira globosa, Bolli (1957), p. 111, pl. 24, figs. 9a–10c

Dentoglobigerina globosa, Wade et al. (2018), p. 348–350, pl. 11.6

Remarks: Fox and Wade (2013) did not record spine holes in the wall texture of *D. globosa* (fig. 5.6c), whereas Wade et al. (2018) did not illustrate SEM wall texture images for this species (pl. 11.6). In this report, we document the first evidence of spine holes in specimen S7 (Plate **P7H**). Two spine holes are found in its edge view, isolated in the last chamber and close to an intersection with two other chambers. However, no spine holes are observed in specimen S8 in Plate **P8**, despite the good preservation. Recrystallization (Plate

P9G, **P9H**) and dissolution (Plate **P9I**) obscure the identification of spine holes in specimen S9, illustrated in Plate **P9**. Pustules are observed in the apertural area of specimen S8 from Hole U1489D (Plate **P8G**), although they are not visible in specimens from Hole U1490A (Plates **P7**, **P9**). *D. globosa* was recorded in Zones M3 and M8 and Subzone M9a.

Dentoglobigerina globularis (Bermúdez, 1961)

(Plate **P10**)

Globoquadrina globularis, Bermúdez (1961), p. 1311, pl. 13, figs. 4–6

Dentoglobigerina globularis, Wade et al. (2018), p. 350–352, pl. 11.7

Remarks: Pearson and Wade (2009) did not record any spine hole in the wall texture of *D. globularis* (pl. 3, fig. 2d), whereas Leckie et al. (1993; pl. 3, fig. 4; pl. 2, fig. 8), Wade et al. (2007; pl. 2g, h), and Wade et al. (2018; pl. 11.7) did not illustrate SEM wall texture images for this species. Our study does not show spine holes or pustules in *D. globularis*, though the preservation state of the test is fairly poor because of recrystallization and infilled pores (Plates **P10G–P10I**). *D. globularis* was recorded in Subzone M1b.

Dentoglobigerina tripartita (Koch, 1926)

(Plates **P11**, **P12**, **P13**, **P14**)

Globigerina bulloides var. *tripartita*, Koch (1926), p. 742, fig. 21a–21b

Dentoglobigerina tripartita, Wade et al. (2018), p. 368–371, pl. 11.15

Remarks: Although the preservation of specimen S11 is good, as shown in Plate **P11**, we did not find direct evidence for spine holes in Miocene *D. tripartita*, nor did previous studies (Wade et al., 2018, pl. 11.15; Fox and Wade, 2013, fig. 8–3c). The rather poor preservation of other specimens (Plates **P12**, **P13**, **P14**), as shown by the presence of recrystallization (Plate **P14I**, **P14J**), overgrowth (Plate **P12G**, **P12H**), and dissolution in some parts of the tests (Plate **P13H**), did not allow for the identification of spine holes. Pustules are observed in specimens illustrated in Plates **P11** and **P13**. Specimen 11 displays numerous pustules in its apertural area (Plate **P11A**, **P11D**, **P11G**), and these are aligned down the umbilical suture from the edge view perspective (Plate **P11B**). Specimen 13 shows fewer pustules in the apertural area both from the umbilical and edge view perspectives. Also, specimen S13 in Plate **P13** has a higher spire than typical specimens (Plates **P11**, **P12**, **P14**), and we refer to this specimen as *D. cf. D. tripartita*. *D. tripartita* was found in Subzone M1b and Zones M3, M6, and M8.

Genus *Globoquadrina* (Finlay, 1947)

Globoquadrina dehiscens (Chapman, Parr, and Collins, 1934)

(Plate **P15**)

Globoquadrina dehiscens, Chapman, Parr, and Collins (1934), p. 569, pl. 11, figs. 36a–36c

Globoquadrina dehiscens, Wade et al. (2018), p. 377–380, pl. 11.17

Remarks: No spine holes were observed in *G. dehiscens* by Wade et al. (2018; pl. 11.17) or by Fox and Wade (2013; fig. 9-1c). Our study did not reveal any spine holes in *G. dehiscens* even though the preservation of specimen S15 in Plate **P15** is good as shown by the smooth edges of pores (Plate **P15G–P15J**). Pustules are observed in the apertural area of specimen S15 both from the umbilical and edge view perspectives (Plate **P15D**, **P15E**), similar to its ancestor *Dentoglobigerina*. *G. dehiscens* is recorded in Zone M3.

Plate P1. *Dentoglobigerina baroemoenensis* (S1); Sample 363-U1490A-23H-CC, 18–23 cm; middle Miocene Subzone M9a. Z-stacker images of (A) umbilical view, (B) edge view, and (C) spiral view. Scanning electron microscope (SEM) images of (D) umbilical view, (E) edge view, and (F) spiral view. Wall texture SEM images of (G) umbilical view, (H) edge view, (I) spiral view, and (J) spiral view. Evidence of spine holes. Scale bars = 100 μm (whole specimens) and 10 μm (close-up images).

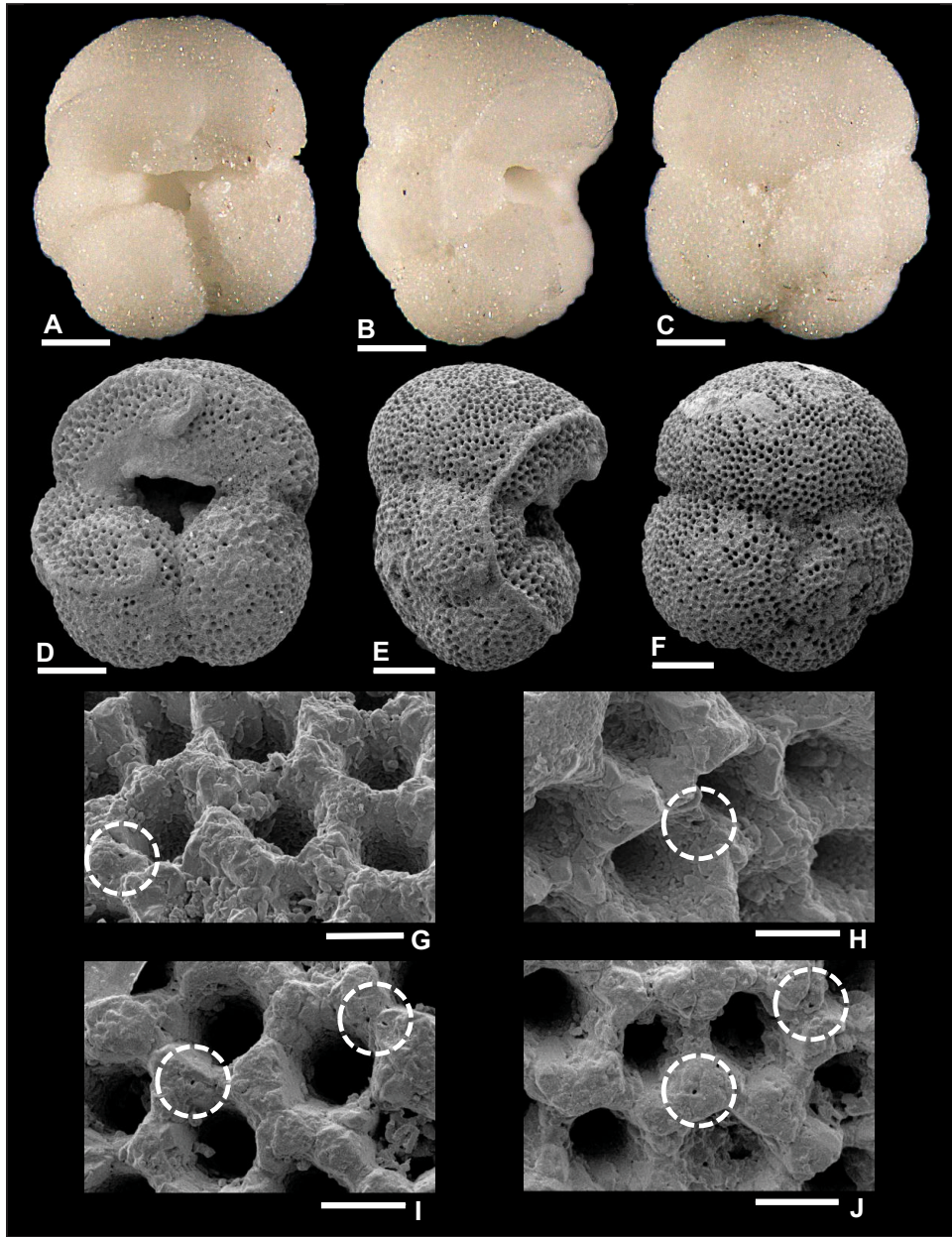


Plate P2. *Dentoglobigerina baroemoensis* (S2); Sample 363-U1490A-24H-CC, 11–16 cm; middle Miocene Zone M8. Z-stacker images of (A) umbilical view, (B) edge view, and (C) spiral view. Scanning electron microscope (SEM) images of (D) umbilical view, (E) edge view, and (F) spiral view. Wall texture SEM images of (G) umbilical view, (H) edge view, and (I) spiral view. Evidence of spine holes. Scale bars = 100 μm (whole specimens) and 10 μm (close-up images).

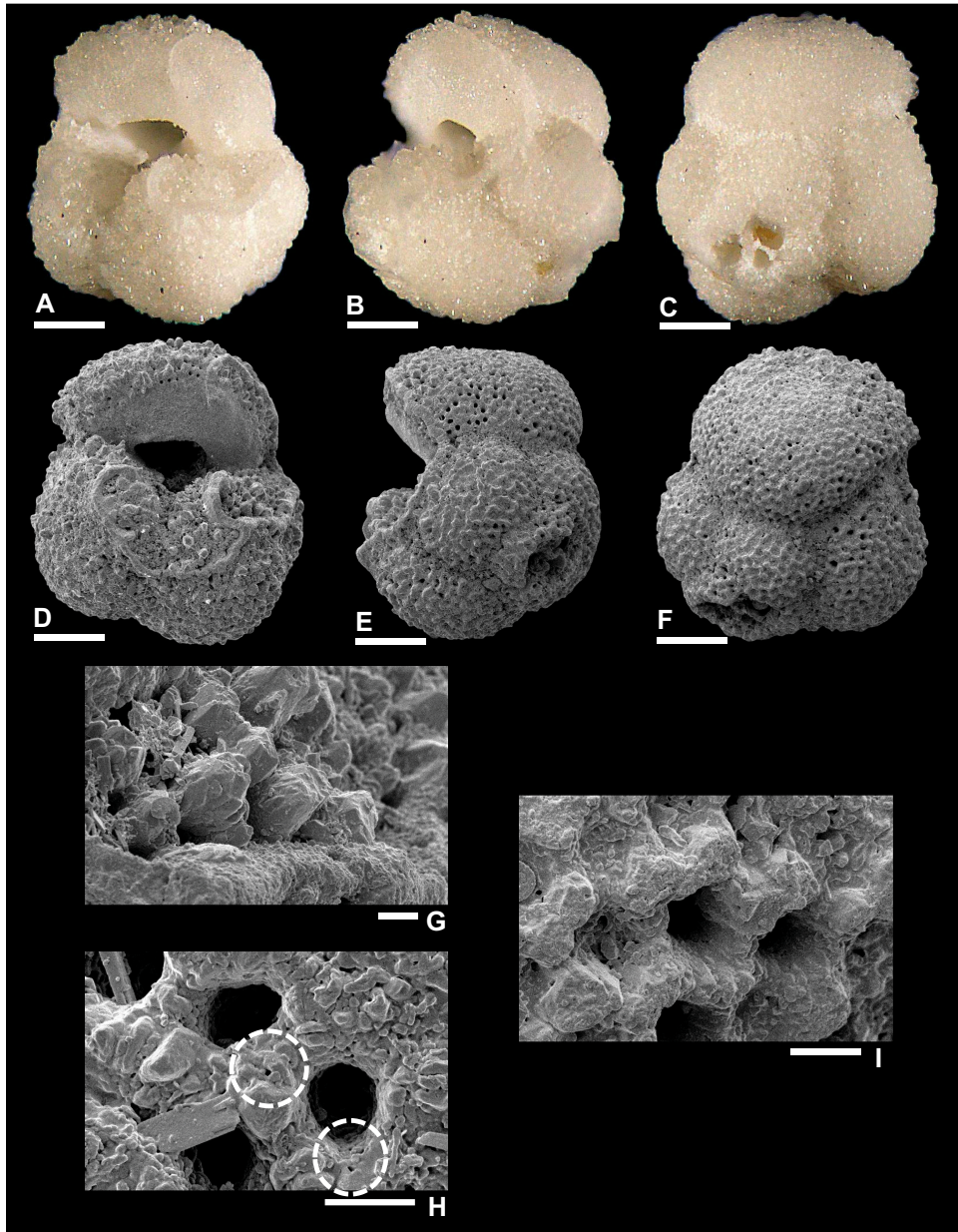


Plate P3. *Dentoglobigerina baroemoenensis* (S3); Sample 363-U1490A-23H-CC, 18–23 cm; middle Miocene Subzone M9a. Z-stacker images of (A) umbilical view, (B) edge view, and (C) spiral view. Scanning electron microscope (SEM) images of (D) umbilical view, (E) edge view, (F) spiral view. Wall texture SEM images of (G) umbilical view and (H) edge view. No evidence of spine holes. Scale bars = 100 μm (whole specimens) and 10 μm (close-up images).

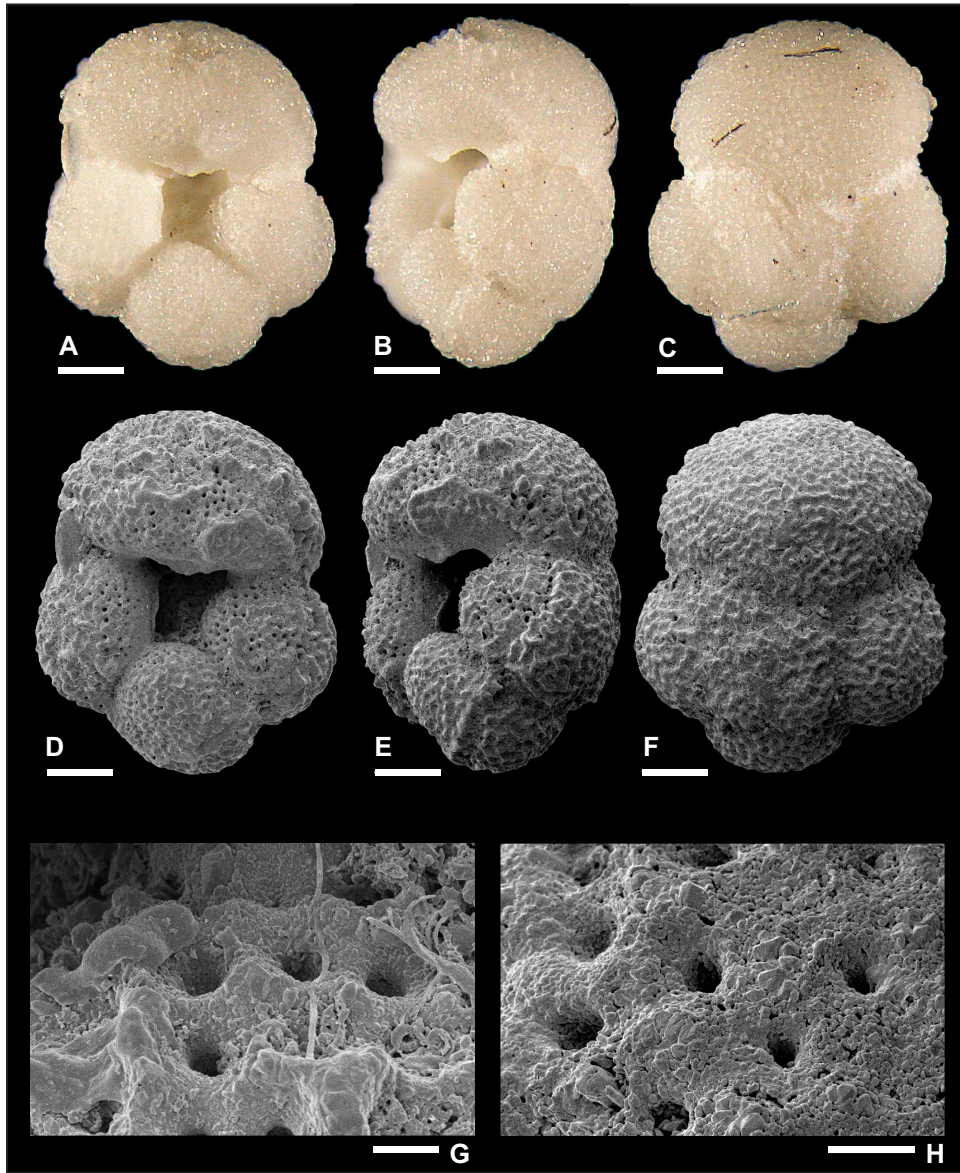


Plate P4. *Dentoglobigerina baroemoenensis* (S4); Sample 363-U1490A-34X-CC, 32–37 cm; lower Miocene Subzone M1b. Z-stacker images of (A) umbilical view, (B) edge view, and (C) spiral view. Scanning electron microscope (SEM) images of (D) umbilical view, (E) edge view, (F) spiral view. Wall texture SEM images of (G) umbilical view and (H) spiral view. No evidence of spine holes. Scale bars: 100 = μm (whole specimens) and 10 μm (close-up images).

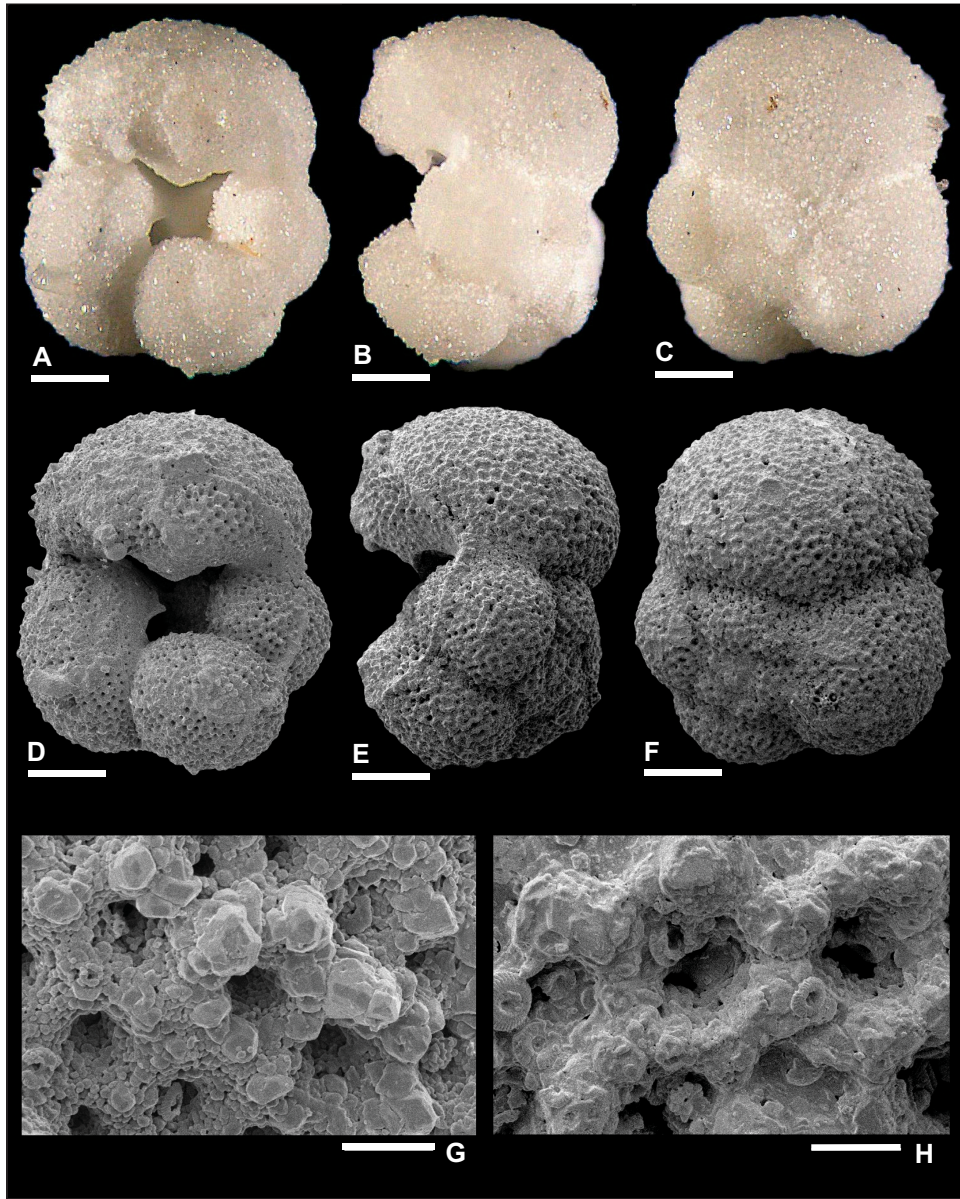


Plate P5. *Dentoglobigerina binaiensis* (S5); Sample 363-U1489D-27X-CC, 18–23 cm; lower Miocene Zone M3. Z-stacker images of (A) umbilical view, (B) edge view, (C) and spiral view. Scanning electron microscope (SEM) images of (D) umbilical view and (E) edge view. Spiral view not obtained. Wall texture SEM images of (F) umbilical view and (G) edge view. No evidence of spine holes. Scale bars = 100 μm (whole specimens) and 10 μm (close-up images).

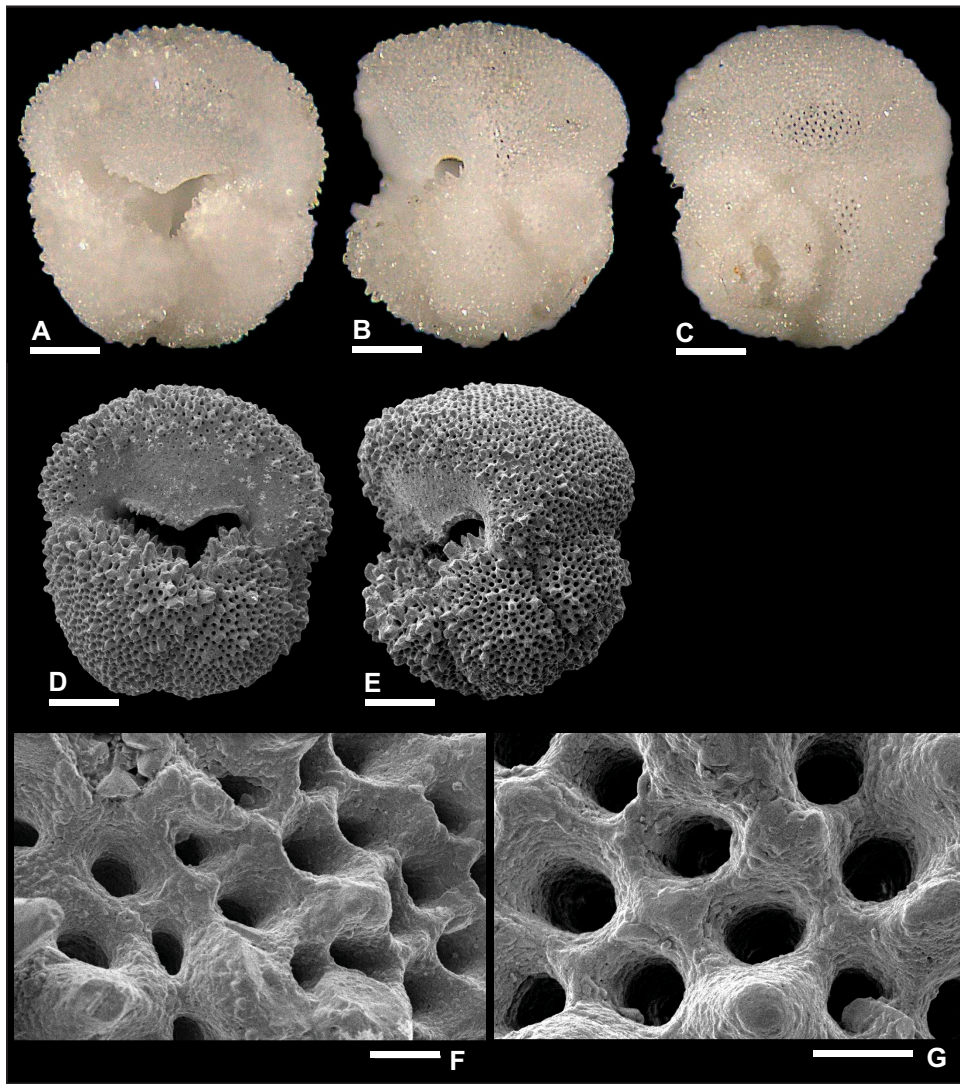


Plate P6. *Dentoglobigerina binaiensis* (S6); Sample 363-U1489D-27X-CC, 18-23 cm; lower Miocene Zone M3. Z-stacker images of (A) umbilical view, (B) edge view, and (C) spiral view. Scanning electron microscope (SEM) images of (D) umbilical view, (E) edge view, and (F) spiral view. Wall texture SEM images of (G) umbilical view, (H) edge view, (I) spiral view, and (J) spiral view. No evidence of spine holes. Scale bars = 100 μm (whole specimens) and 10 μm (close-up images).

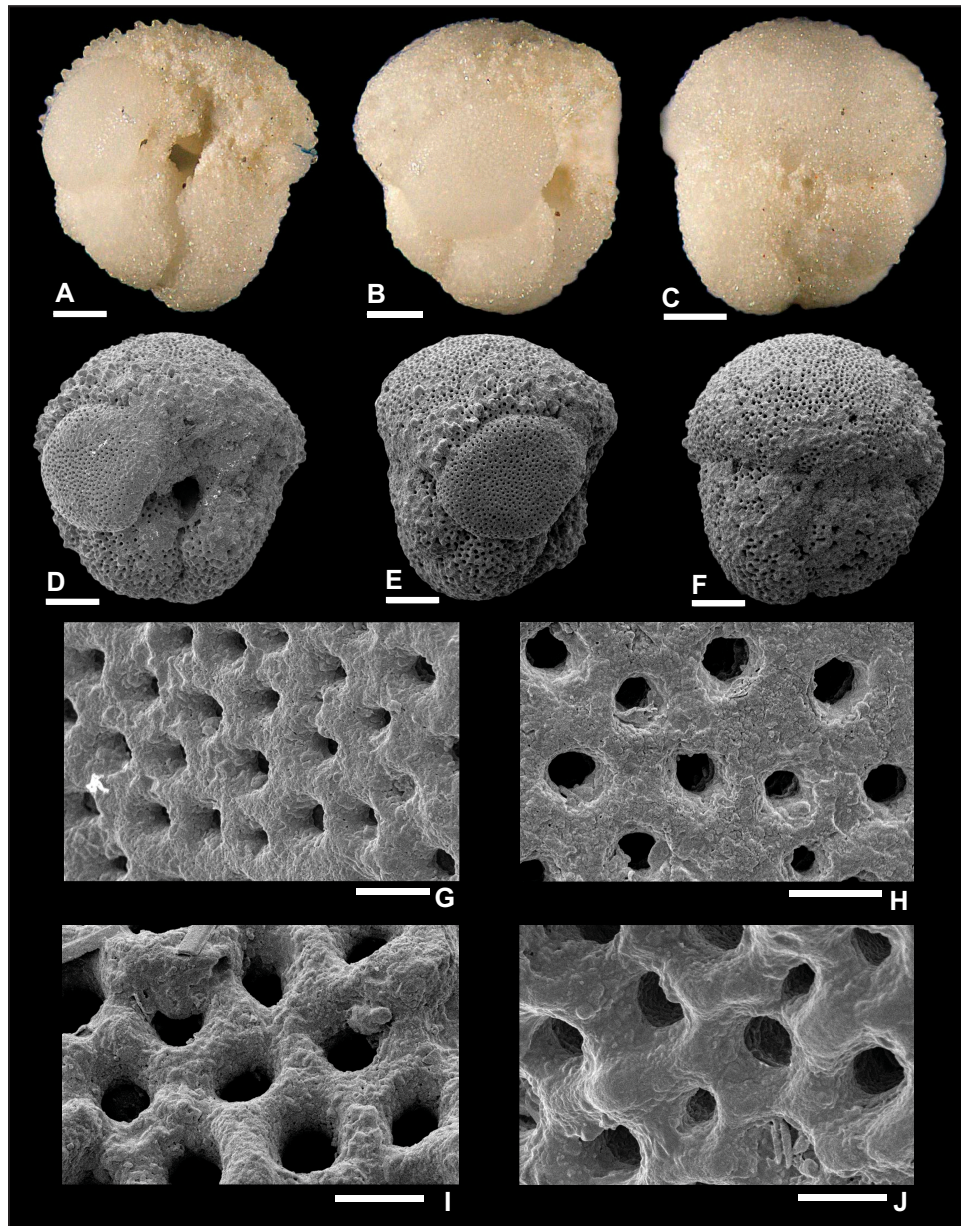


Plate P7. *Dentoglobigerina globosa* (S7); Sample 363-U1490A-23H-CC, 18–23 cm; middle Miocene Subzone M9a. Z-stacker images of (A) umbilical view, (B) edge view, and (C) spiral view. Scanning electron microscope (SEM) images of (D) umbilical view, (E) edge view, and (F) spiral view. Wall texture SEM images of (G) umbilical view, (H) edge view, (I) spiral view, and (J) spiral view. Evidence of possible spine holes. Scale bars = 100 μm (whole specimens) and 10 μm (close-up images).

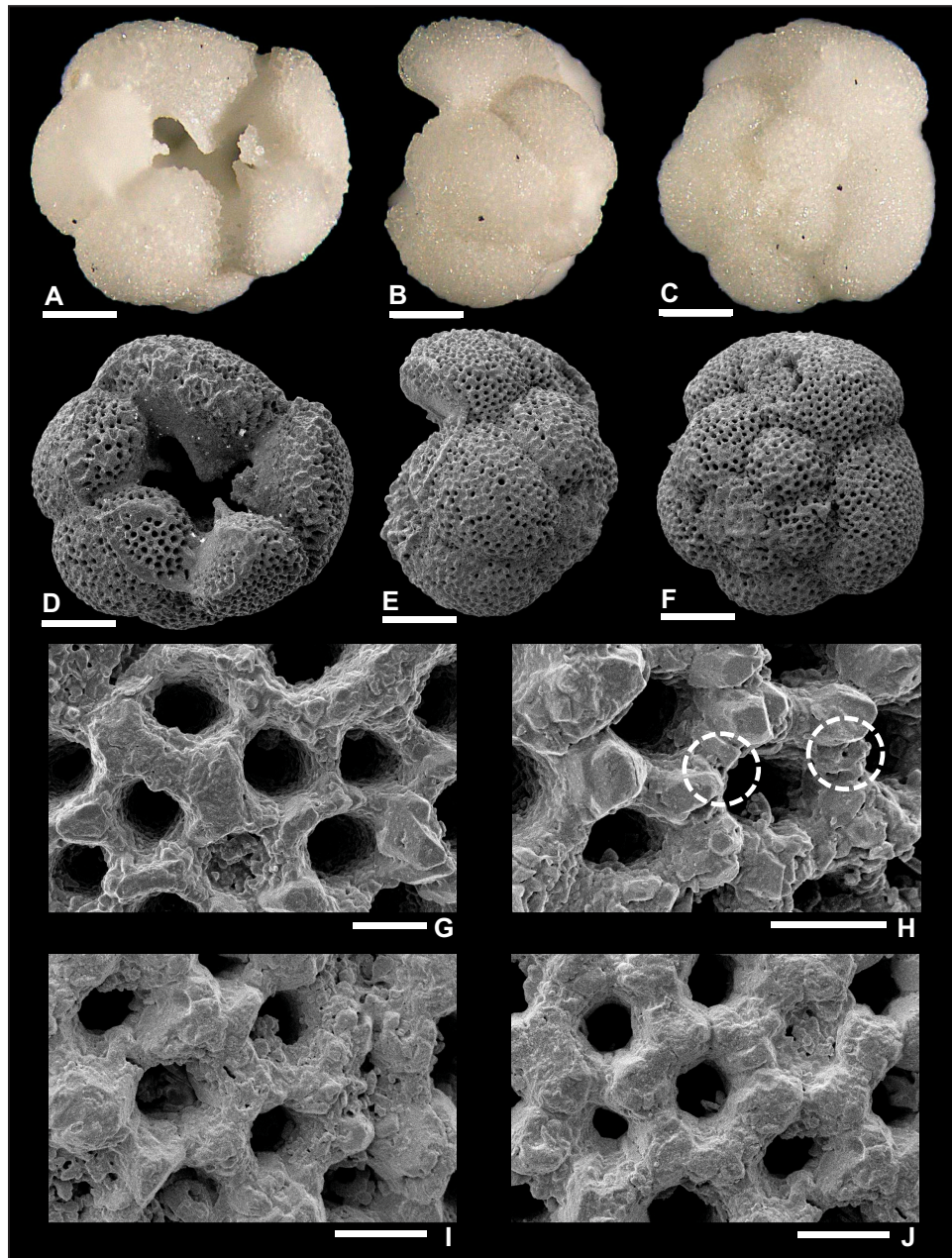


Plate P8. *Dentoglobigerina globosa* (S8); Sample 363-U1489D-27X-CC, 18–23 cm; lower Miocene Zone M3. Z-stacker images of (A) umbilical view, (B) edge view, and (C) spiral view. Scanning electron microscope (SEM) images of (D) umbilical view, (E) edge view, and (F) spiral view. Wall texture SEM images of (G) umbilical view, (H) edge view, (I) spiral view, and (J) spiral view. No evidence of spine holes. Scale bars = 100 μm (whole specimens) and 10 μm (close-up images).

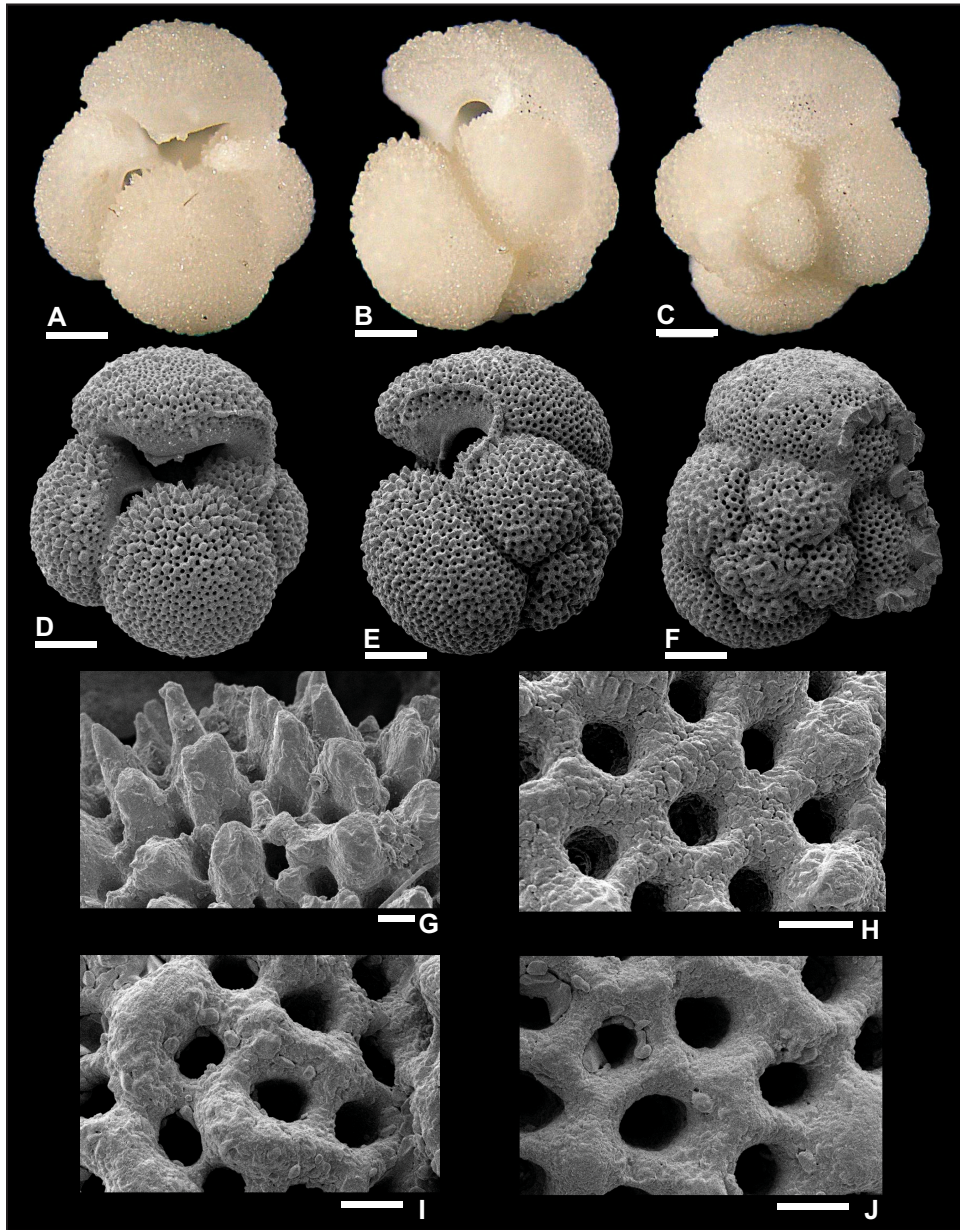


Plate P9. *Dentoglobigerina globosa* (S9); Sample 363-U1490A-24H-CC, 11–16 cm; middle Miocene Zone M8. Z-stacker images of (A) umbilical view, (B) edge view, and (C) spiral view. Scanning electron microscope (SEM) images of (D) umbilical view, (E) edge view, and (F) spiral view. Wall texture SEM images of (G) umbilical view, (H) edge view, and (I) spiral view. No evidence of spine holes. Scale bars = 100 μm (whole specimens) and 10 μm (close-up images).

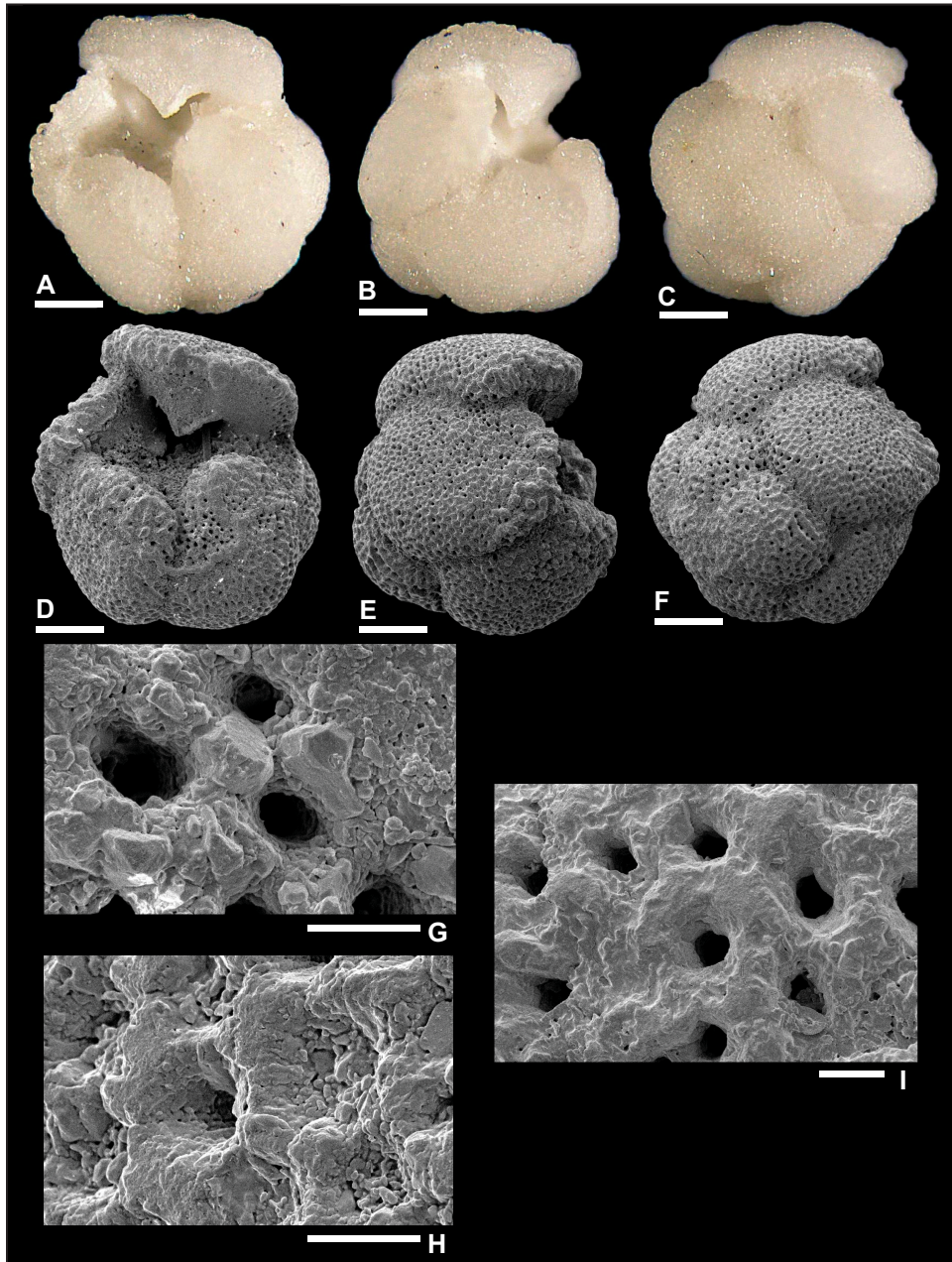


Plate P10. *Dentoglobigerina globularis* (S10); Sample 363-U1490A-34X-CC, 32–37 cm; lower Miocene Subzone M1b. Z-stacker images of (A) umbilical view, (B) edge view, and (C) spiral view. Scanning electron microscope (SEM) images of (D) umbilical view, (E) edge view, and (F) spiral view. Wall texture SEM images of (G) umbilical view, (H) edge view, and (I) spiral view. No evidence of spine holes. Scale bars = 100 μm (whole specimens) and 10 μm (close-up images).

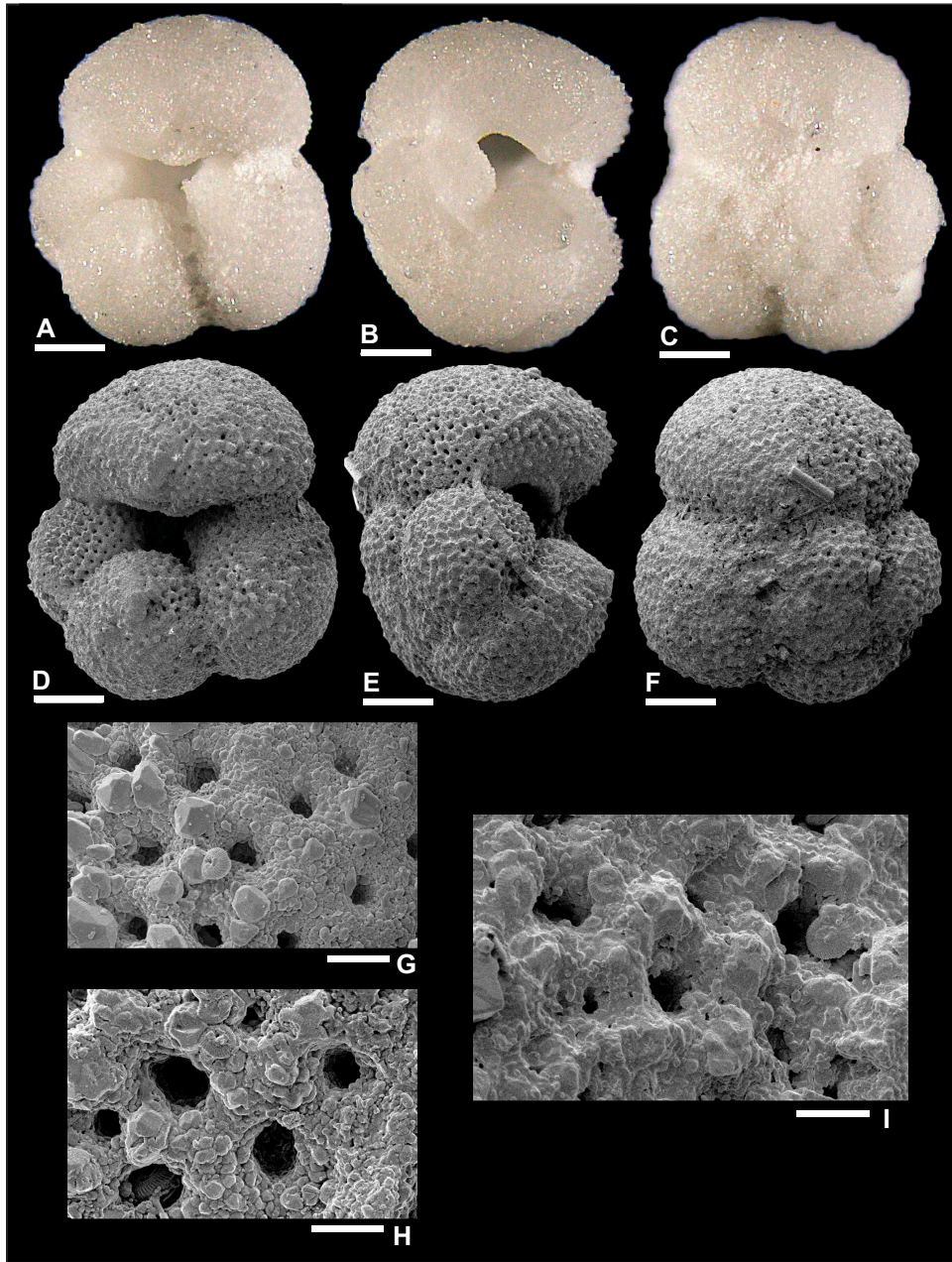


Plate P11. *Dentoglobigerina tripartita* (S11); Sample 363-U1489D-27X-CC, 18–23 cm; lower Miocene Zone M3. Z-stacker images of (A) umbilical view, (B) edge view, and (C) spiral view. Scanning electron microscope (SEM) images of (D) umbilical view, (E) edge view, and (F) spiral view. Wall texture SEM images of (G) umbilical view, (H) edge view, (I) spiral view, and (J) spiral view. No evidence of spine holes. Scale bars = 100 μm (whole specimens) and 10 μm (close-up images).

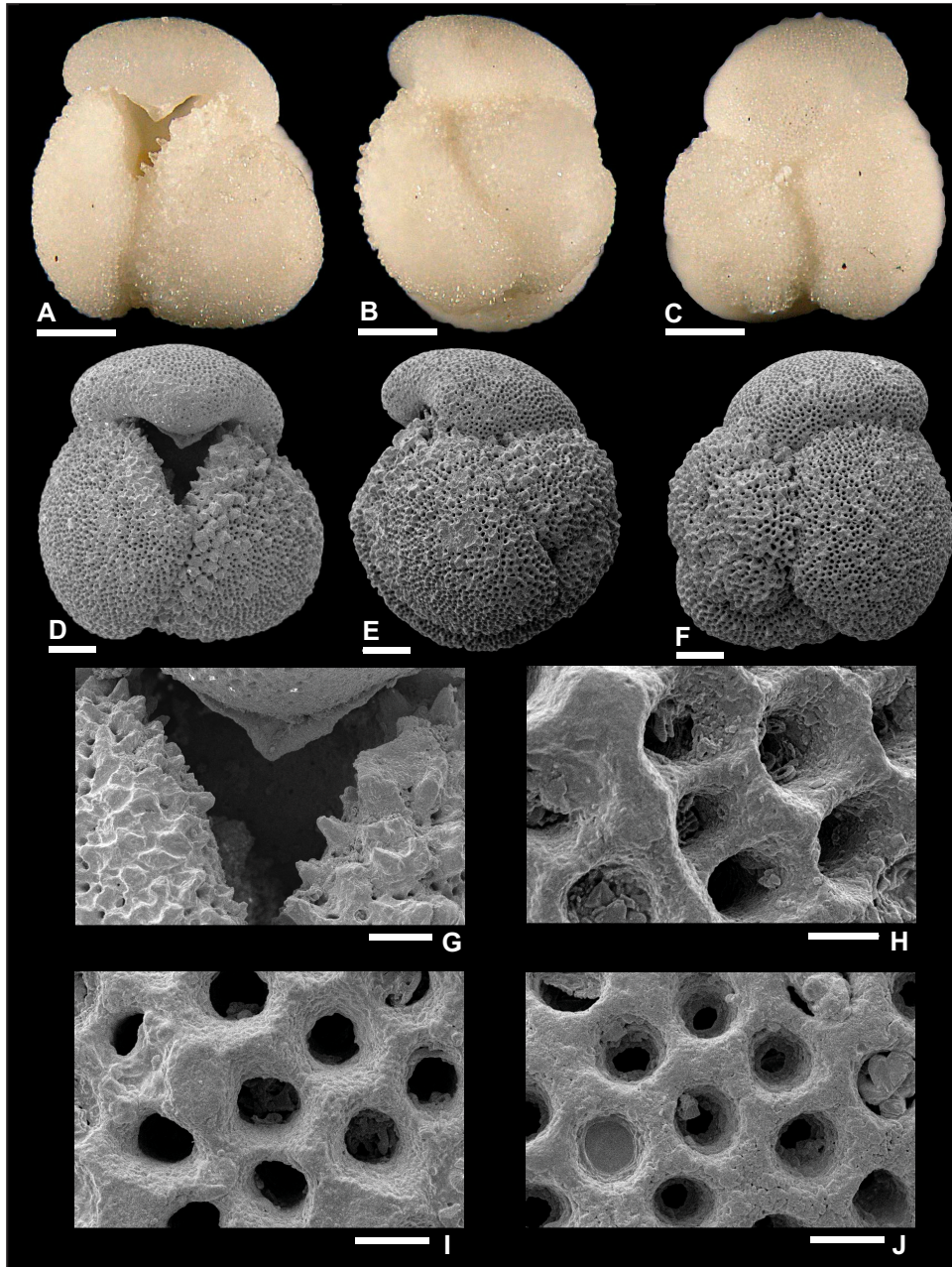


Plate P12. *Dentoglobigerina tripartita* (S12); Sample 363-U1490A-24H-CC, 11–16 cm; middle Miocene Zone M8. Z-stacker images of (A) umbilical view, (B) edge view, and (C) spiral view. Scanning electron microscope (SEM) images of (D) umbilical view, (E) edge view, and (F) spiral view. Wall texture SEM images of (G) umbilical view and (H) edge view. No evidence of spine holes. Scale bars = 100 μm (whole specimens) and 10 μm (close-up images).

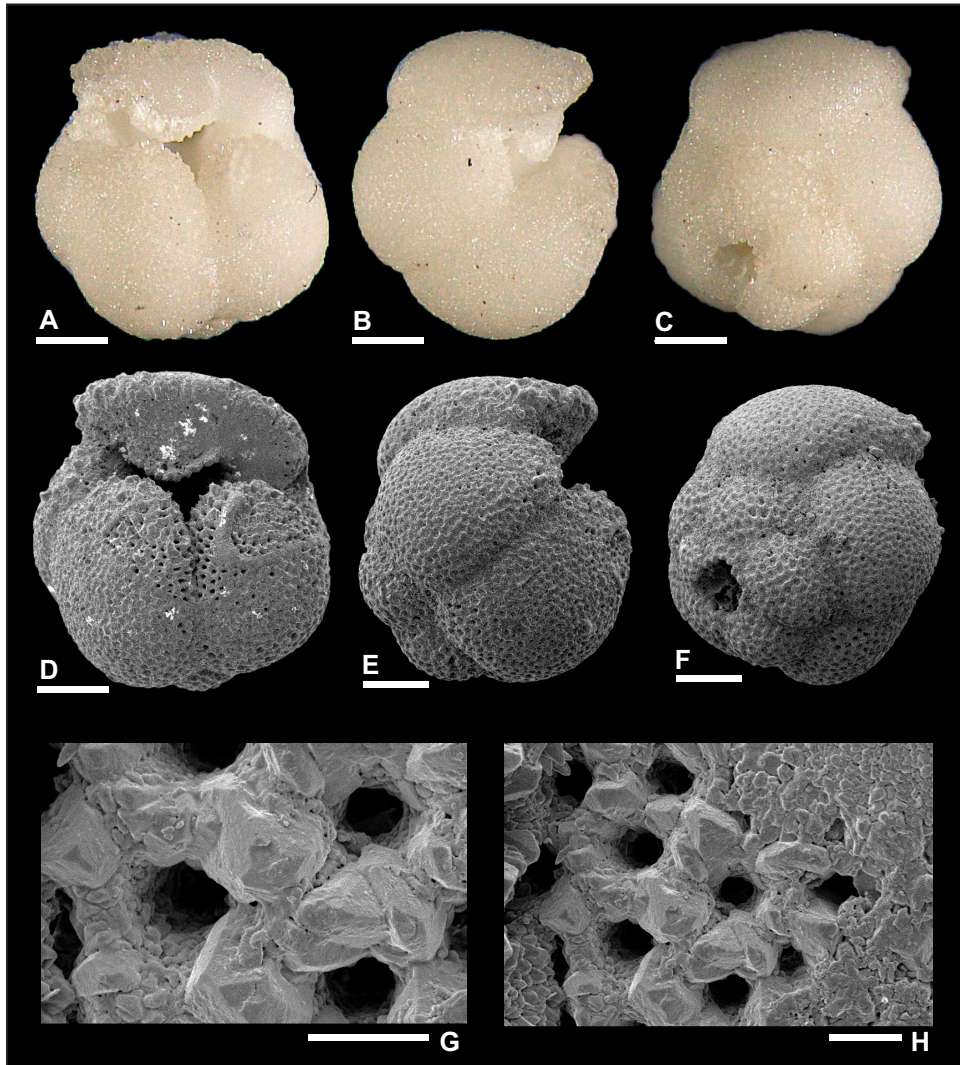


Plate P13. *Dentoglobigerina* cf. *D. tripartita* (S13); Sample 363-U1490A-25H-CC, 16–21 cm; lower–middle Miocene Zone M6. Z-stacker images of (A) umbilical view, (B) edge view, and (C) spiral view. Scanning electron microscope (SEM) images of (D) umbilical view, (E) edge view, and (F) spiral view. Wall texture SEM images of (G) umbilical view and (H) edge view. No evidence of spine holes. Scale bars = 100 μm (whole specimens) and 10 μm (close-up images).

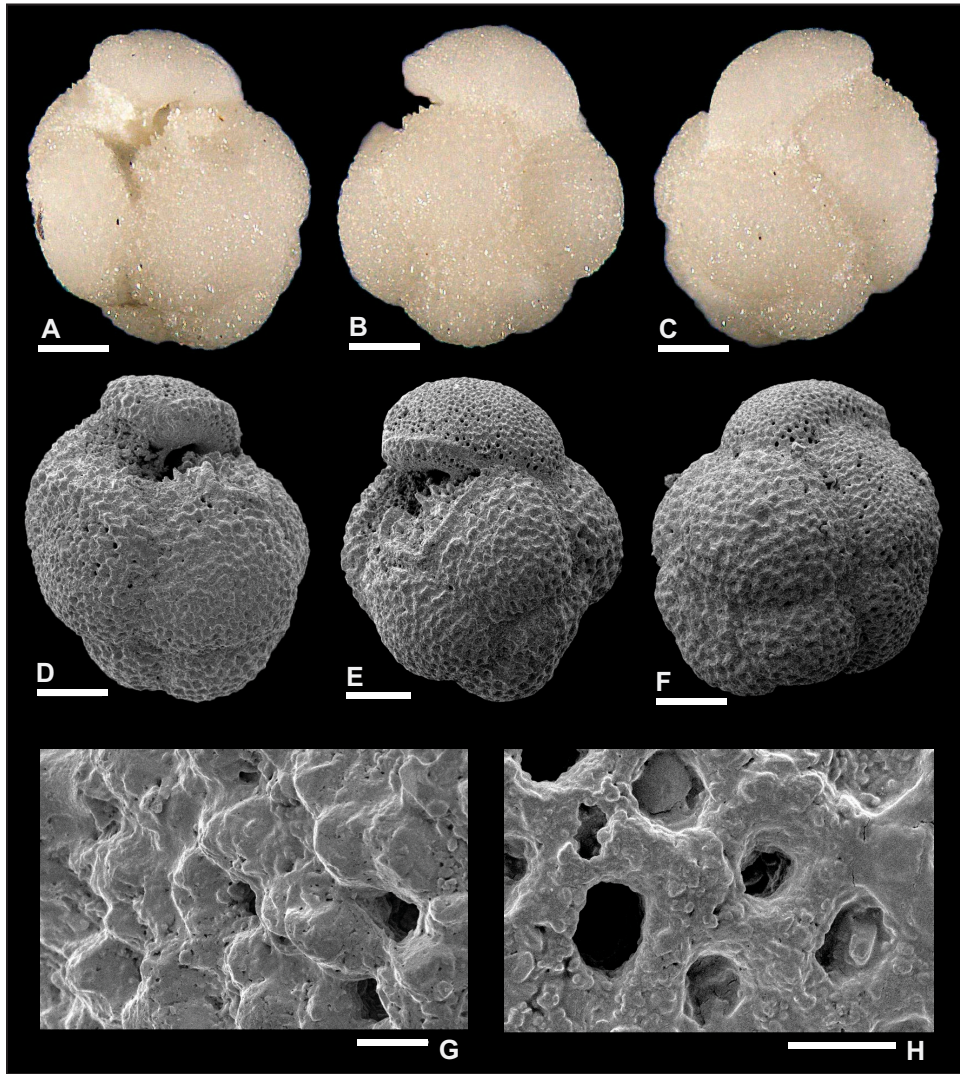


Plate P14. *Dentoglobigerina tripartita* (S14); Sample 363-U1490A-34X-CC, 32–37 cm; lower Miocene Subzone M1b. Z-stacker images of (A) umbilical view, (B) edge view, and (C) spiral view. Scanning electron microscope (SEM) images of (D) umbilical view, (E) edge view, and (F) spiral view. Wall texture SEM images of (G) umbilical view, (H) edge view, (I) spiral view, and (J) spiral view. No evidence of spine holes. Scale bars = 100 μm (whole specimens) and 10 μm (close-up images).

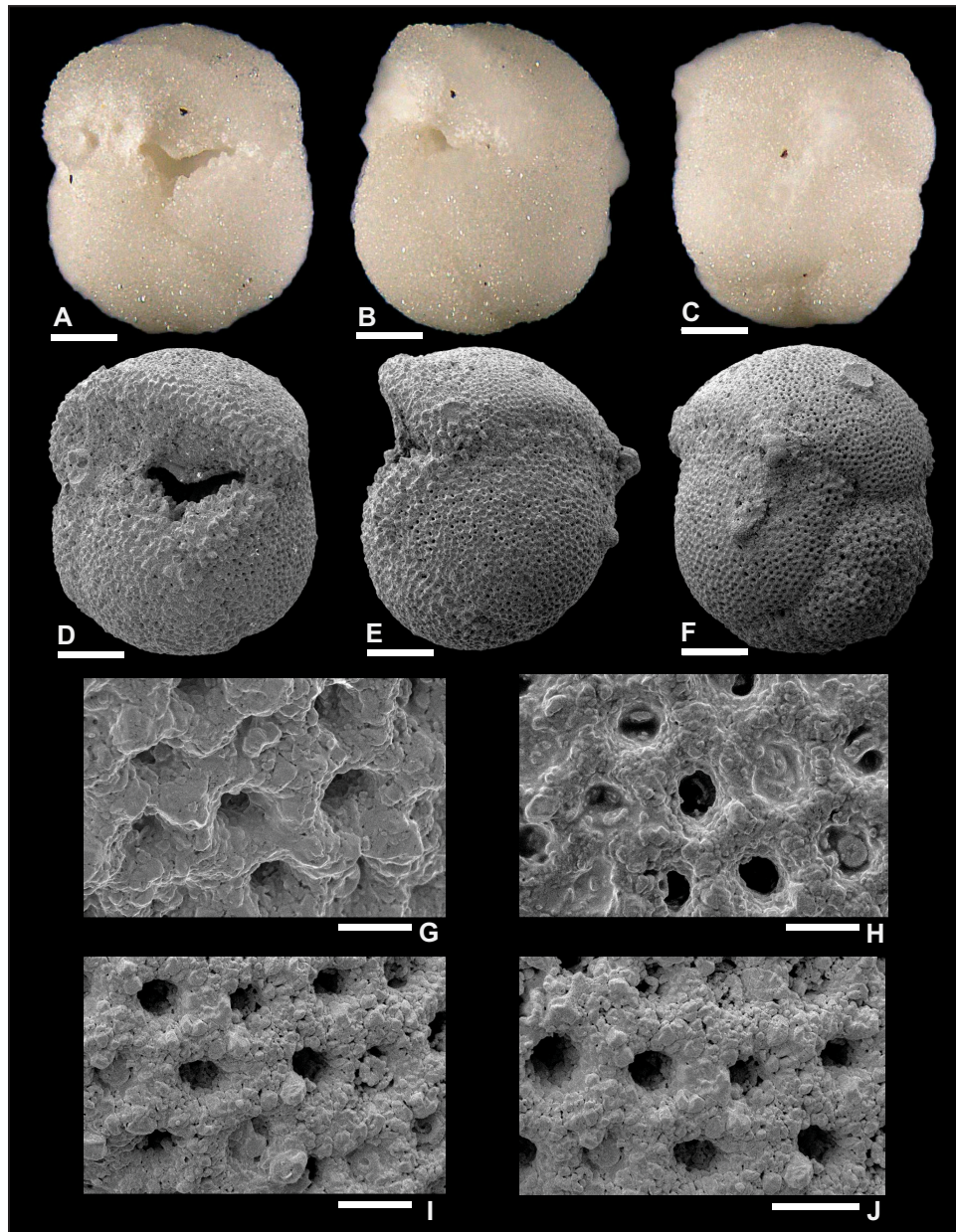


Plate P15. *Globoquadrina dehiscens* (S15); Sample 363-U1489D-27X-CC, 18–23 cm; lower Miocene Zone M3. Z-stacker images of (A) umbilical view, (B) edge view, and (C) spiral view. Scanning electron microscope (SEM) images of (D) umbilical view, (E) edge view, and (F) spiral view. Wall texture SEM images of (G) umbilical view, (H) edge view, (I) spiral view, and (J) spiral view. No evidence of spine holes. Scale bars = 100 μm (whole specimens) and 10 μm (close-up images).

